Int. J.Nano Dimens. 5(2): 187-196, Spring 2014
ISSN: 2008-8868

Contents list available at **IJND**

International Journal of Nano Dimension

Journal homepage: *www.IJND.ir*

Static and modal analysis of parabolic-boundary functionalized Carbon nanotube-reinforced composite plates using FEM

M. H. Shojaeefard
A. Khalkhali*
SH. Khakshournia
F. Malmir

School of automotive engineering, Iran university of science and technology, Tehran, Iran.

Received: 03 December 2012
Accepted: 21 February 2013

ABSTRACT

This paper investigates the effect of different methods of carbon nanotubes distribution in a thin matrix on static and dynamic behavior of the nanocomposite. Five different symmetric patterns of distribution are considered, including four parabolic patterns and a linear one. For each pattern, the effective mechanical properties of the resultant nanocomposite are calculated using the rule of mixture. Influence of geometric parameters on static and free vibration responses of the nanocomposite plate are studied. Finite element modeling is created using Abaqus/CAE. The resulting responses for linear distribution of nanotubes are compared to a past work and good agreement is observed between them. The finite element simulations showed that in all different cases of geometric parameters, the value of non-dimensional static deflection of the mid-point of plate under a uniformly distributed load is minimized in the linear distribution pattern of carbon nanotubes case and will increase by changing the pattern to a parabola. This fact is vice versa about modal analysis. Linear distribution pattern of carbon nanotubes results in higher natural frequencies in comparison with the parabolic distributions of carbon nanotubes.

Keywords: *Carbon nanotube; Composite plate; Vibration; Finite element method; Functionally graded.*

* Corresponding author:
A. Khalkhali
School of automotive engineering, Iran university of science and technology, Tehran, Iran.
Tel +98 9303030339
Fax +98 2188221285
Email ab_khalkhali@iust.ac.ir

INTRODUCTION

Severe competition for producing more effective and simultaneously more economical productions has made companies use novel materials instead of the old and classic ones. One of these prevalent novel materials is carbon nanotube (CNT). Carbon nanotubes have significant mechanical and electrical properties owing to their weird high ratio of length to diameter [1-3].

It has been shown that it is possible to reach the same mechanical properties which we expect by addition of a certain value of micro-scaled reinforce materials, if we add a remarkable less value of carbon nanotubes to the same polymer matrix [4-5].

Functionally graded materials (FGMs) are novel composite materials which the microstructural details are spatially varied through non-uniform distribution of the reinforcement phase [6-7]. Carbon nanotube reinforced composite (CNTRC) plates with functionally distribution of carbon nanotubes are widely being studied in recent years. For instance Hui Shen Shen et al [6] analysied thermal buckling and postbuckling behavior of these composite plates. They showed that the buckling temperature as well as thermal postbuckling strength of the plate can be increased as a result of functionally graded reinforcement.

Distribution pattern of carbon nanotubes in the base polymer matrix plate, is clearly effictive on the mechanical properties of final composite material. In a comparison of four different linear distribution patterns of carbon nanotubes by Ping Zhu et al.[8], as it is shown in Figure 1 it was concluded that if functionalization takes place as Figure 2, the central deflection of carbon nanotube reinforced composite (CNTRC) plate will be minimum and the natural frequencies are more than the corresponding values for other linear patterns of distribution. It is clear that the difference in static and vibration responses originates from the difference in mechanical properties in the different patterns of functionalization[9],[10]. Due to production limitations of functionally graded CNTRC plates in our desired pattern of functionalization, we may face to some deviations from our desired distribution pattern of the reinforcement. In this paper we are about to investigate the effect of these deviations on the macroscopic responses of CNTRC plates. This challenge is investigated using four parabolic-boundaries of CNTs distribution patterns around the desired linear patterrn.

Ping Zhu and his colleagues used a combination of MD simulations and the rule of mixture developed for nanocomposites materials. The difference between the rule of mixture for simple composite and nanocomposite materilas is in nano-reinforcement efficiency factor. This factor is related to the orientation, length and volume fraction of the reinforcement phase and specially to the bond strength between the matrix and reinforcement phase. A common method to find this factor in different directions is to combine MD simulations or representative volume element method (RVE) with the rule of mixture. If we match the young moduli in longitudinal and transverse direction and the shear moduli for a certain volume fraction calculated using MD simulations or continuum models like RVE to the counterparts computed by the rule of mixture, the CNT efficiency parameters would be found.

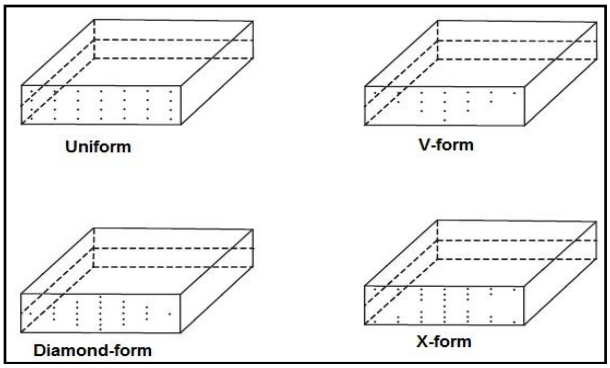

Fig. 1. Four different linear distribution patterns of CNTs, considered by Ping Zhu et al. [8]

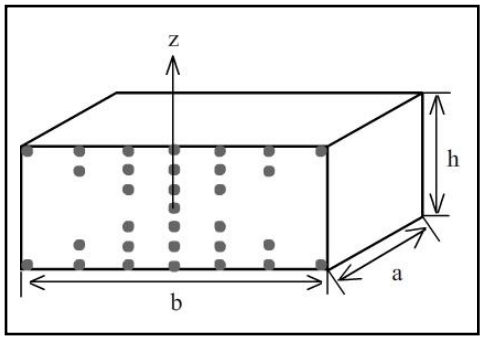

Fig. 2. X-form linear distribution of carbon nanotubes in a CNTRC plate

In this paper, dispersion of CNTs are considered as equal for all the cases through the width of nanocomposite plate (*a* in Figure 2). Due to functionally distribution of CNTs, the volume fraction of reinforcement in each elevation through *z*-axis will be different. In other words, the volume fractions of reinforcement and matrix phase are a function of *z*. Three cases of CNT volume fractions

are studied in this paper. We used the CNT efficiency parameters calculated in [8] for each case of CNT volume fractions. The effective mechanical properties of CNTRC plate for each z value are calculated using the rule of mixture and mentioned efficiency parameters. Then, the macroscopic simulations including static and vibration analysis are carried out using FEM by ABAQUS/CAE. The plate is assumed to be thin, therefore we will have a plane stress analysis.

EXPERIMENTAL

Distribution patterns

Five different symmetric patterns of distribution are considered in this paper, including four parabolic patterns and a linear one as depicted in Figure 3. The linear and four parabolic patterns of functionally graded distributions of carbon nanotubes along the thickness direction of the nanocomposite plates are assumed to be as following for *h=2 mm*:

$$V_{CNT}(z) = \left(19.74\sqrt{8|z| + 0.0001} - 0.197\right)V_{CNT}^{*} \quad Para1$$

$$V_{CNT}(z) = \left(44.12\sqrt{4|z| + 0.0009} - 1.324\right)V_{CNT}^{*} \quad Para2$$

$$V_{CNT}(z) = 2000|z|V_{CNT}^{*} \quad Linear$$

$$V_{CNT}(z) = \left(8.15\sqrt{-4|z| + 0.005} + 0.571\right)V_{CNT}^{*} \quad Para3$$

$$V_{CNT}(z) = \left(6.64\sqrt{-8|z| + 0.008} + 0.597\right)V_{CNT}^{*} \quad Para3$$

(1a)

Where

$$V_{CNT}^{*} = \frac{W_{CNT}}{W_{CNT} + \left(\frac{\rho^{CNT}}{\rho^{m}}\right) - \left(\frac{\rho^{CNT}}{\rho^{m}}\right)W_{CNT}}$$

(1b)

Where W_{CNT} is the mass fraction of carbon nanotubes in the composite plate, and ρ^{m} and ρ^{CNT} are the densities of matrix and CNT respectively. V_{CNT}^{*} is the volume fraction of carbon nanotubes in the composite plate if carbon nanotubes have been dispersed uniformly in the volume of CNTRC plate. V_{CNT} is the volume fraction of carbon nanotubes for each supposed function of dispersion. Equation 1 shows that the volume fraction varies with z. Hence we have to divide the composite plate into different layers in z-direction. In order to simplifying the calculations, we suppose that distribution of carbon nanotubes is uniform through each layer. In this paper, we considered 10 layers for each plate.

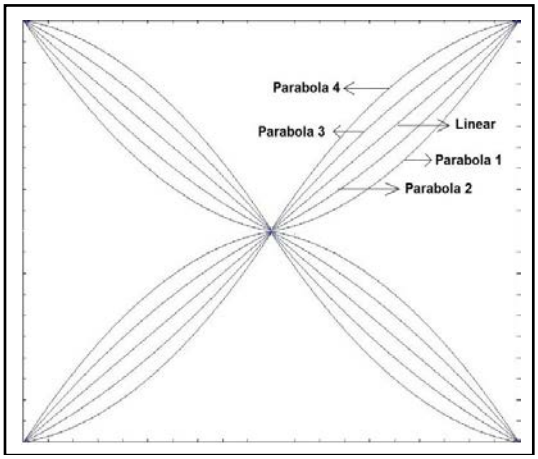

Fig. 3. Supposed distribution patterns of carbon nanotubes in CNTRC plates

The rule of mixture for CNTRC materials

The effective material properties of the two-phase nanocomposites, mixture of CNTs and an isotropic matrix can be estimated according to the rule of mixture [11], [12]. We can write the equations of mixture as:

$$E_{11} = \eta_1 V_{CNT} E_{11}^{CNT} + V_m E^m \quad \textbf{(2a)}$$

$$\frac{\eta_2}{E_{22}} = \frac{V_{CNT}}{E_{22}^{CNT}} + \frac{V_m}{E^m} \quad \textbf{(2b)}$$

$$\frac{\eta_3}{G_{12}} = \frac{V_{CNT}}{G_{12}^{CNT}} + \frac{V_m}{G^m} \quad \textbf{(2c)}$$

$$\upsilon_{12} = V_{CNT}^{*}\upsilon_{12}^{CNT} + V_m\upsilon^m \quad \textbf{(2d)}$$

$$\rho = V_{CNT}\rho^{CNT} + V_m\rho^m \quad \textbf{(2e)}$$

Where, V_m is the volume fraction of isotropic matrix and E_{11}, G_{12} represent the Young and Shear modulus of CNTRC plate in the relevant

directions. υ_{12} and ρ^m are the Poisson's ratios. υ_{12} is considered as constant over the thickness of the functionally graded CNTRC plates. η_j (j = 1,2,3) represents the effect of quality of dispersion and the length of nanotubes through the volume of isotropic matrix[8],[13].

RESULTS AND DISCUSSION

In the present paper, a is considered to have the same value as b, and b/h ratio varies from 10 to 20 and to 50. Four boundary conditions are considered for the static analysis. CCCC, SSSS, SCSC and SFSF which represent fully clamped, fully simply supported, clamped and simply supported, simply supported and free respectively. The only considered case for modal analysis is the CCCC boundary conditions case. h is supposed to be 2 milimeters. Three cases are considered for V_{CNT}^* in static analysis and only one case in modal analysis. For the case of V_{CNT}^* = 0.11, η_1 = 0.149 and η_2 = 0.934. For the case of V_{CNT}^* = 0.14, η_1 = 0.150 and η_2 = 0.941. For the case of V_{CNT}^* = 0.17, η_1 = 0.149 and η_2 = 1.381.[8] In addition we assume that $\eta_2 = \eta_3$ and $G_{12} = G_{13} = G_{23}$. PmPv is considered as the matrix. The material properties of PmPv are assumed to be $\upsilon^m = 0.34$, $\rho^m = 1150 kg/m^3$ and $E^m = 2.1\ GPa$ at room temperature [14]. The mechanical properties of single-walled carbon nanotube (10,10) is considered as $\upsilon_{12}^{CNT} = 0.175$, $E_{11}^{CNT} = 5.6466\ TPa$, $E_{22}^{CNT} = 7.0800\ Tpa$, $G_{12}^{CNT} = 1.9445\ TPa$ and $\rho^{CNT} = 1400\ Kg/m^3$[15].

The mid-point static deflactions of CNTRC plates are illustrated in Table 1 for different volume fractions and width to height ratios under different boundary conditions. Further the six non-dimensional natural frequencies under CCCC boundary conditions $\bar{\omega} = \omega(\frac{a^2}{h})\sqrt{\rho^m/E^m}$ found by Abaqus/CAE simulations are represented in Table 2. All the data for the linear distribution case are compared with a past work done by Ping Zhu et al.[8]. Whole of the compared values have reasonable and good agreement together. Maximum difference between the two cases (Present and Ping Zhu) is 5% which arises from difference in element types, number of supposed layers for the CNTRC plate and meshing method.

Figure 4 shows the first six natural mode shapes of a CNTRC plate for the case of *b/h=0.17* and distribution pattern of parabola 4 under fully clamped boundary conditions. The horizontal axes in Figures 5 to 11 represent the different types of carbon nanotubes distribution. As it is shown in Figures 5 to 8, the minimum central deflection pertains to the linear pattern of distribution. Farther, the central deflection difference between the linear pattern and parabola 3 is obviously more than the difference between the central deflection of the linear pattern and parabola 2. Hence we can conclude that if the distribution pattern of carbon nanotubes, deviates from linear to downward parabola pattern, we must expect a big jump in central deflection in comparison to upward parabola cases. As we see in Figure 3, carbon nanotubes in downward parabola patterns are more compressed than the upward ones. Therefore, compressing carbon nanotubes from the linear distribution pattern leads to a rather high increase in the central deflection of CNTRC plates.

Comparison of corresponding figures of different boundary conditions shows that the proportion of deflections related to different volume fractions, are higher in the case of CCCC boundary condition. Also for a distinct boundary condition, addition of width to thickness ratio, leads to produce lower proportion of central deflections of different volume fractions. Compression of three different volume fraction graphs by increasing the width to thickness ratio for each boundary condition proves this fact.

The trend is vice versa for the natural frequency case. Figures 9 to 11 illustrate this issue that as the distribution diverges from the linear pattern, the natural frequency will decrease. The simulations results represented in Table 2 approve this fact. The other important result is the difference between the effect of downward deviations from the linear distribution and upward deviations. The effect of upward deviations in increasing the mid-point static deflection and decreasing the natural frequencies are remarkably more than downward deviations effects. Therefore, compressing carbon nanotubes from the linear distribution pattern leads to a rather high decrease in the natural frequencies of CNTRC plates.

Also comparison of Figures 9 to 11 shows that increasing the natural frequency number, will not have a remarkable affect on the proportion of natural frequencies related to different *b/h* ratios.

Table 1. Effect of distribution pattern of carbon nanotubes and volume fraction V_{CNT}^{*} and b/h ratio on the non-dimensional central deflection $\bar{w} = -w_0/h$ for CNTRC plates under a uniformly distributed load $q_0 = -0.1Mpa$ and four different boundary conditions.

V_{CNT}^{*}	b/h	Distribution	CCCC Present	CCCC Ping Zhu	SSSS Present	SSSS Ping Zhu	SCSC Present	SCSC Ping Zhu	SFSF Present	SFSF Ping Zhu
0.11	10	Parabola 1	2.12E-3		3.33E-3		2.99E-3		3.13E-3	
		Parabola 2	2.11E-3		3.25E-3		2.92E-3		3.05E-3	
		Linear	2.10E-3	2.11E-3	3.18E-3	3.18E-3	2.86E-3	2.87E-3	2.98E-3	2.91E-3
		Parabola 3	2.25E-3		3.89E-3		3.43E-3		3.72E-3	
		Parabola 4	2.27E-3		3.96E-3		3.49E-3		3.80E-3	
	20	Parabola 1	1.20E-2		2.95E-2		2.81E-2		2.80E-2	
		Parabola 2	1.17E-2		2.83E-2		2.70E-2		2.68E-2	
		Linear	1.15E-2	1.15E-2	2.72E-2	2.70E-2	2.61E-2	2.59E-2	2.57E-2	2.48E-2
		Parabola 3	1.38E-2		3.85E-2		3.58E-2		3.70E-2	
		Parabola 4	1.41E-2		3.96E-2		3.68E-2		3.82E-2	
	50	Parabola 1	0.209		0.889		0.865		0.854	
		Parabola 2	0.199		0.839		0.820		0.806	
		Linear	0.191	0.189	0.797	0.790	0.781	0.773	0.766	0.734
		Parabola 3	0.278		1.239		1.174		1.199	
		Parabola 4	0.287		1.282		1.211		1.243	
0.14	10	Parabola 1	2.02E-3		3.00E-3		2.71E-3		2.80E-3	
		Parabola 2	2.01E-3		2.94E-3		2.66E-3		2.74E-3	
		Linear	1.99E-3	1.98E-3	2.88E-3	2.88E-3	2.61E-3	2.58E-3	2.68E-3	2.59E-3
		Parabola 3	2.11E-3		3.44E-3		3.07E-3		3.25E-3	
		Parabola 4	2.13E-3		3.50E-3		3.12E-3		3.31E-3	
	20	Parabola 1	1.09E-2		2.47E-2		2.39E-2		2.34E-2	
		Parabola 2	1.07E-2		2.37E-2		2.30E-2		2.24E-2	
		Linear	1.05E-2	1.04E-2	2.29E-2	2.26E-2	2.22E-2	2.18E-2	2.16E-2	2.08E-2
		Parabola 3	1.23E-2		3.19E-2		3.02E-2		3.04E-2	
		Parabola 4	1.25E-2		3.28E-2		3.10E-2		3.13E-2	
	50	Parabola 1	0.173		0.707		0.698		0.680	
		Parabola 2	0.166		0.668		0.661		0.642	
		Linear	0.159	0.156	0.635	0.627	0.630	0.621	0.610	0.585
		Parabola 3	0.227		0.988		0.954		0.952	
		Parabola 4	0.234		1.023		0.985		0.986	
0.17	10	Parabola 1	1.36E-3		2.16E-3		1.93E-3		2.03E-3	
		Parabola 2	1.36E-3		2.11E-3		1.89E-3		1.98E-3	
		Linear	1.35E-3	1.32E-3	2.07E-3	2.01E-3	1.85E-3	1.80E-3	1.94E-3	1.84E-3
		Parabola 3	1.43E-3		2.50E-3		2.21E-3		2.39E-3	
		Parabola 4	1.44E-3		2.55E-3		2.24E-3		2.45E-3	
	20	Parabola 1	7.77E-3		1.93E-2		1.83E-2		1.83E-2	
		Parabola 2	7.62E-3		1.85E-2		1.76E-2		1.75E-2	
		Linear	7.48E-3	7.29E-3	1.78E-2	1.74E-2	1.69E-2	1.65E-2	1.68E-2	1.60E-2
		Parabola 3	8.90E-3		2.51E-2		2.33E-2		2.44E-2	
		Parabola 4	9.06E-3		2.58E-2		2.39E-2		2.49E-2	
	50	Parabola 1	0.136		0.583		0.564		0.559	
		Parabola 2	0.130		0.550		0.535		0.527	
		Linear	0.125	0.122	0.523	0.513	0.510	0.499	0.500	0.476
		Parabola 3	0.182		0.813		0.768		0.786	
		Parabola 4	0.187		0.841		0.792		0.815	

Table 2. Effect of distribution pattern of carbon nanotubes and volume fraction V_{CNT}^{*} and b/h ratio on the first six non-dimensional natural frequencies $\bar{\omega} = \omega(\frac{a^2}{h})\sqrt{\rho^m/E^m}$ of CNTRC square fully clamped (CCCC) plates.

V_{CNT}^{*}	b/h	Mode number	Parabola 1	Parabola 2	Linear Present	Linear Ping Zhu	Parabola 3	Parabola 4
0.11	10	1	17.98	18.05	18.13	18.08	17.52	17.44
		2	23.34	23.42	23.51	23.61	22.87	22.80
		3	33.56	33.66	33.77	34.34	33.08	33.02
		4	34.25	34.37	34.51	34.47	33.47	33.33
		5	37.49	37.51	37.49	37.45	36.78	36.65
		6	37.53	37.65	37.79	37.79	37.43	37.43
	20	1	29.89	30.19	30.48	30.42	27.99	27.75
		2	34.50	34.79	35.07	35.04	32.75	32.54
		3	45.88	46.18	46.47	46.48	44.27	44.09
		4	61.34	61.75	62.17	61.98	58.62	58.23
		5	63.91	64.32	64.73	64.56	61.15	60.93
		6	64.43	64.75	65.07	65.17	62.83	62.67
	50	1	44.12	45.12	46.03	46.17	38.57	38.00
		2	47.90	48.85	49.71	49.93	42.73	42.22
		3	58.25	59.11	59.91	60.23	53.72	53.28
		4	77.58	78.39	79.16	79.53	73.55	73.18
		5	106.65	107.48	108.28	108.65	95.87	94.63
		6	107.14	109.06	110.81	110.92	98.00	96.80
0.14	10	1	18.35	18.41	18.47	18.59	17.98	17.91
		2	23.78	23.87	23.96	24.24	23.33	23.26
		3	34.15	34.27	34.40	35.22	33.61	33.55
		4	34.92	35.00	35.11	35.41	34.32	34.20
		5	38.04	38.08	38.13	38.17	37.60	37.48
		6	38.22	38.32	38.45	38.79	37.95	37.96
	20	1	31.16	31.42	31.67	31.86	29.46	29.23
		2	35.73	36.01	36.28	36.49	34.07	33.87
		3	47.15	47.47	47.79	48.09	45.46	45.27
		4	63.27	63.61	63.97	64.33	60.96	60.60
		5	65.81	66.16	66.40	66.91	63.54	63.20
		6	65.89	66.28	66.68	67.15	64.03	63.85
	50	1	48.10	49.13	50.07	50.40	42.27	41.67
		2	51.67	52.67	53.58	54.03	46.14	45.58
		3	61.68	62.64	63.52	64.11	56.64	56.15
		4	80.79	81.75	82.65	83.39	76.07	75.63
		5	109.93	110.97	111.98	112.90	103.72	102.47
		6	114.83	116.69	118.38	119.13	105.09	104.43
0.17	10	1	22.28	22.35	22.43	22.75	21.82	21.74
		2	29.10	29.22	29.36	29.88	28.47	28.39
		3	41.98	42.15	42.36	43.29	41.19	41.11
		4	42.37	42.45	42.58	43.56	41.73	41.58
		5	46.57	46.68	46.84	47.07	45.84	45.70
		6	46.83	46.90	47.00	47.61	46.66	46.67
	20	1	36.93	37.27	37.59	38.06	34.70	34.41
		2	42.86	43.23	43.60	44.11	40.64	40.38
		3	57.37	57.83	58.31	58.93	55.00	54.75
		4	75.77	76.19	76.63	77.64	72.88	72.44
		5	79.10	79.54	80.00	81.04	76.22	75.79
		6	80.83	81.42	82.04	82.93	78.11	77.86
	50	1	51.98	55.53	56.64	57.25	47.46	46.76
		2	59.19	60.39	61.49	62.24	52.69	52.04
		3	72.51	73.70	74.82	75.75	66.43	65.86
		4	97.21	98.49	99.72	100.85	91.18	90.65
		5	131.94	134.24	136.33	137.91	118.27	116.77
		6	134.12	135.60	137.08	138.49	120.95	119.48

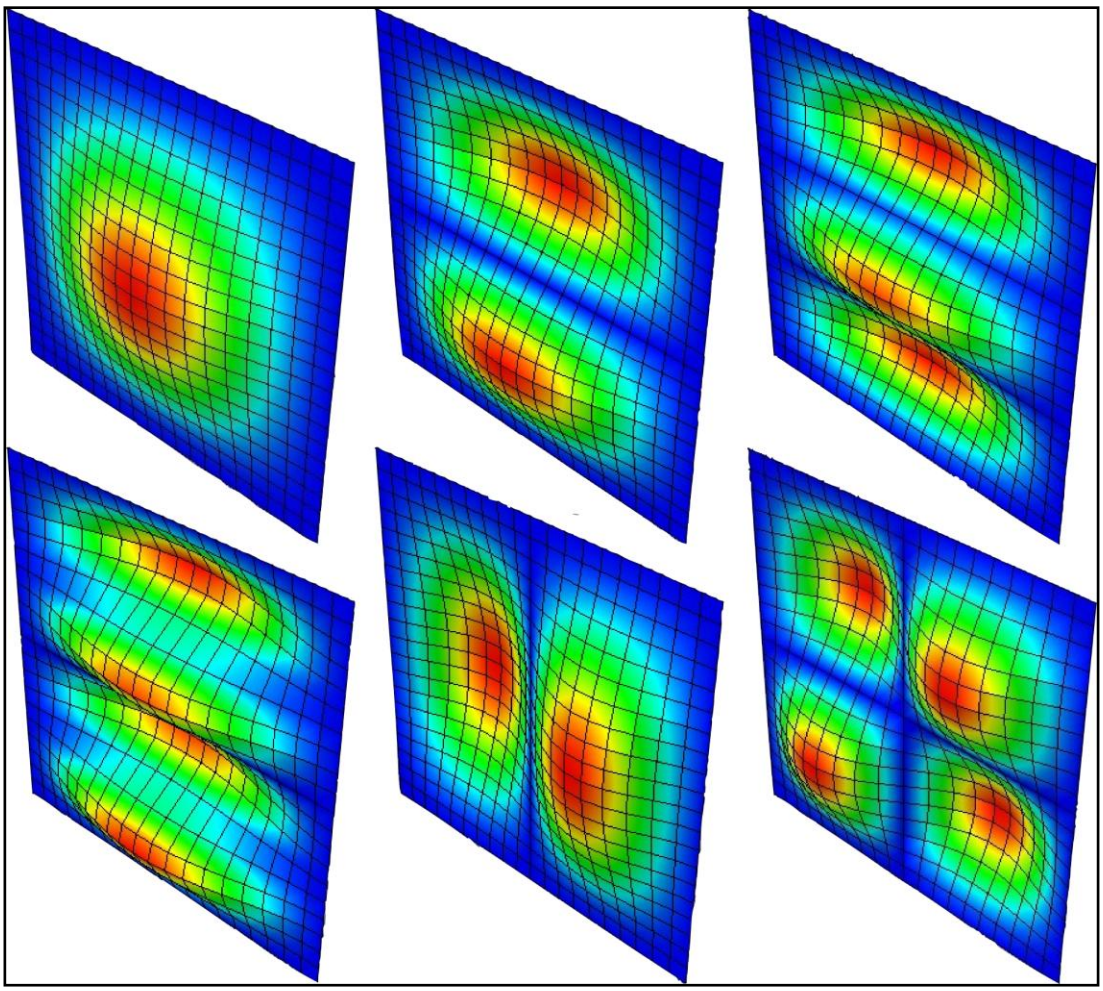

Fig. 4. Six first natural mode shapes of a CNTRC plate while b/h=0.17 (Parabola 4) , (CCCC)

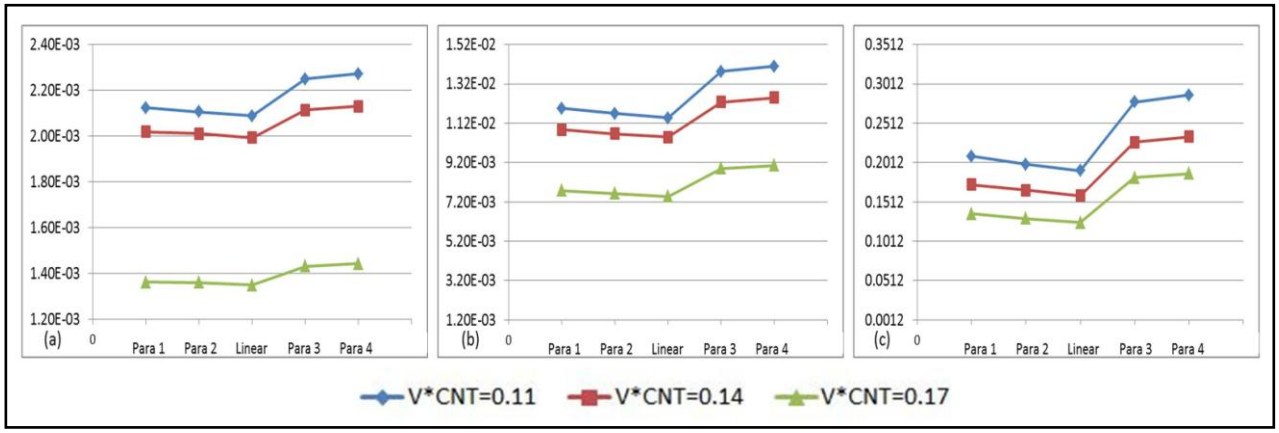

Fig. 5. Variations of central deflection of plate with different distribution pattens under CCCC boundary conditions for: (a) *b/h=10*, (b) *b/h=20*, (c) *b/h=50*

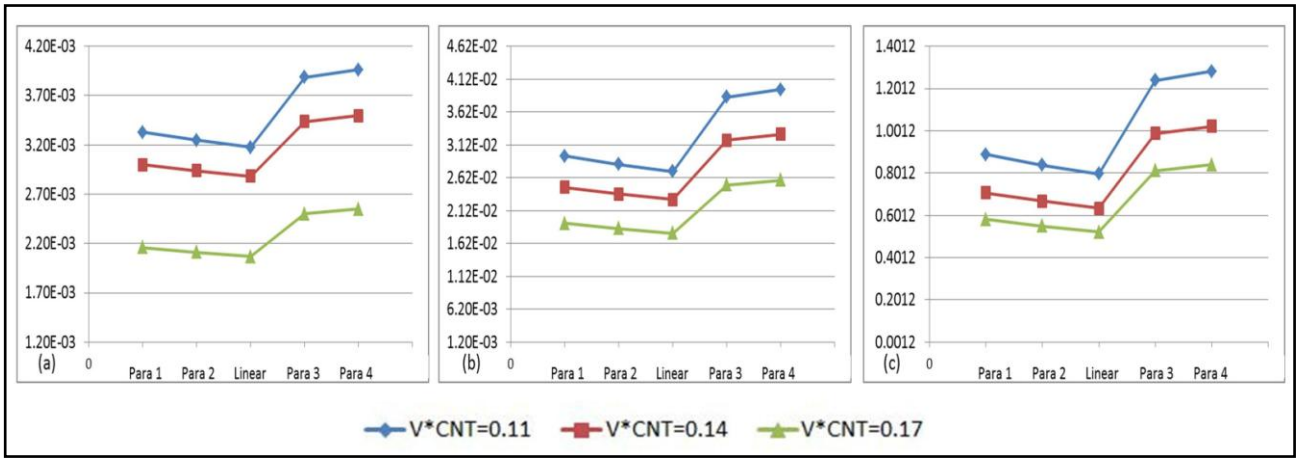

Fig. 6. Variations of central deflection of plate with different distribution pattens under SSSS boundary conditions for: (a) *b/h=10*, (b) *b/h=20*, (c) *b/h=50*

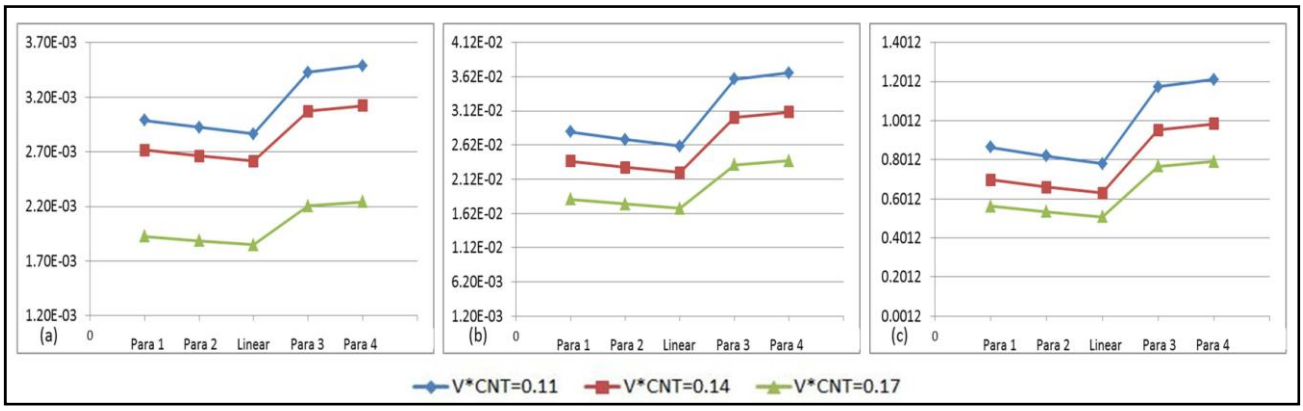

Fig. 7. Variations of central deflection of plate with different distribution pattens under SCSC boundary conditions for: (a) *b/h=10*, (b) *b/h=20*, (c) *b/h=50*

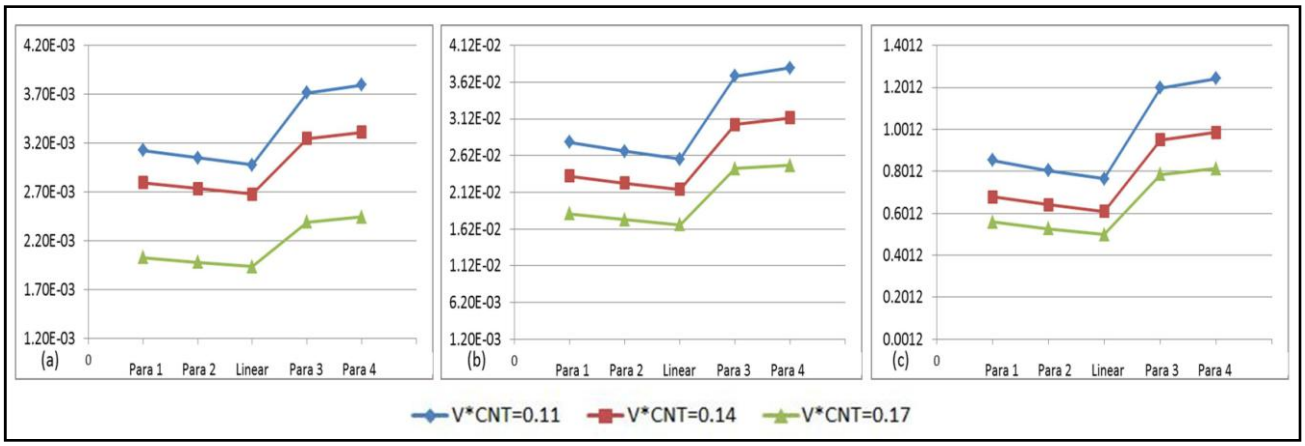

Fig. 8. Variations of central deflection of plate with different distribution pattens under SFSF boundary conditions for: (a) *b/h=10*, (b) *b/h=20*, (c) *b/h=50*

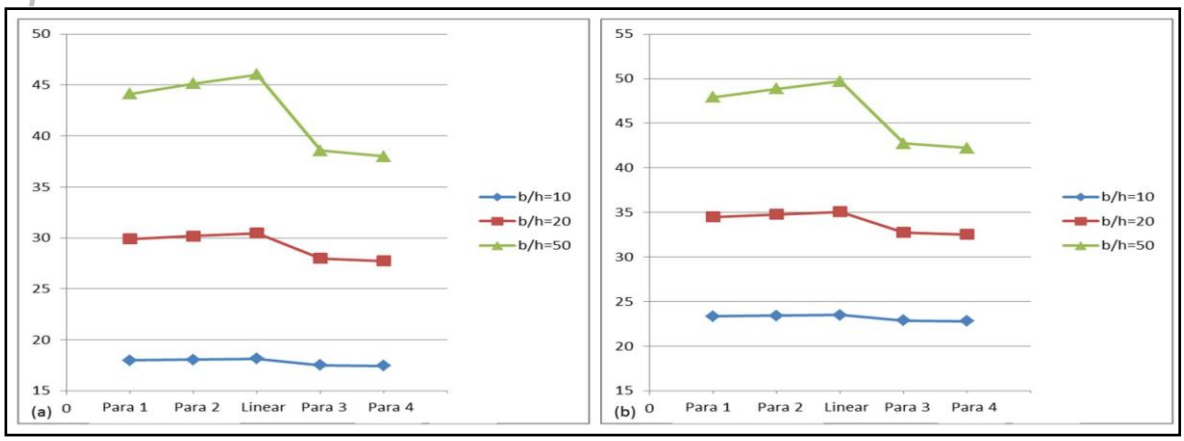

Fig. 9. Variations of (a) first and (b) second natural frequencies of CNTRC plate with different distribution patterns under CCCC boundary conditions while V_{CNT}^{*}=0.11

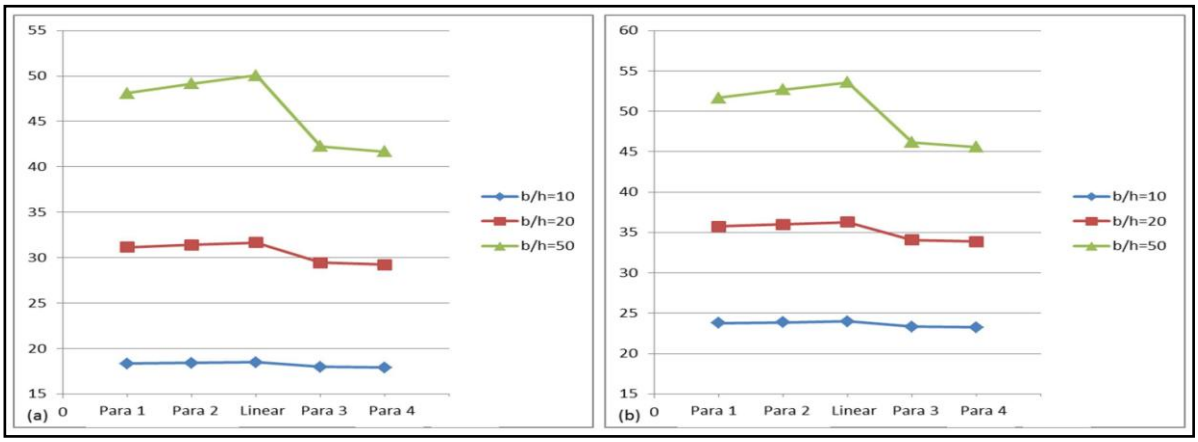

Fig. 10. Variations of (a) first and (b) second natural frequencies of CNTRC plate with different distribution patterns under CCCC boundary conditions while V_{CNT}^{*}=0.14

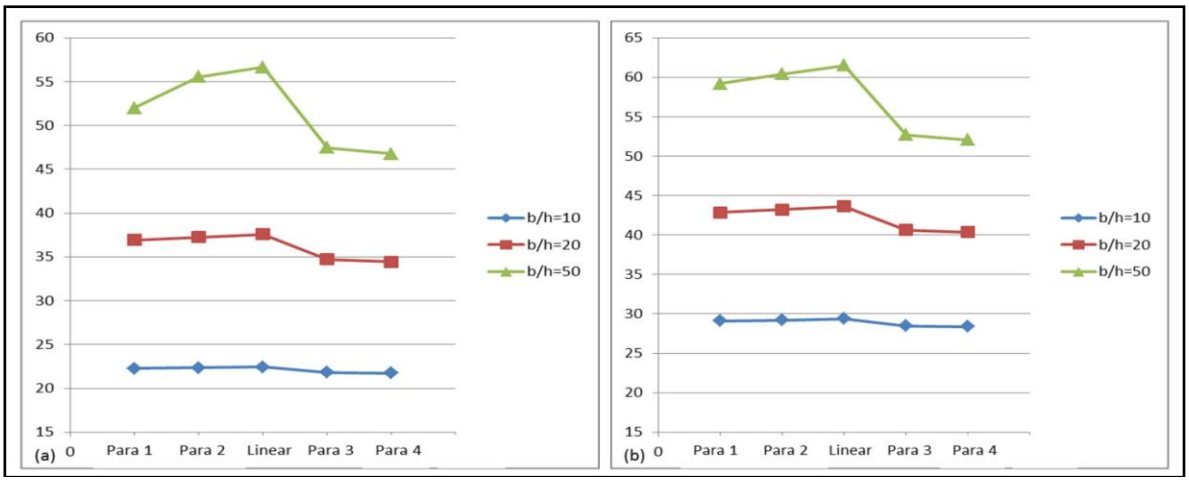

Fig. 11. Variations of (a) first and (b) second natural frequencies of CNTRC plate with different distribution patterns under CCCC boundary conditions while V_{CNT}^{*}=0.17

CONCLUSIONS

In this paper we investigated the effect of carbon nanotubes distribution patterns and the geometric parameters of a CNTRC plate under different boundary conditions on static and modal responses of these plates. Numerical simulations showed that the linear distribution pattern leads to the minimum central deflection and the maximum natural frequencies. Further, the effect of upward deviations in distribution pattern of carbon nanotubes which is equal to compressing carbon nanotubes are remarkably more than downward deviations effects which is equal to dispersion of carbon nanotubes in the isotropic matrix.

REFERENCES

[1] Wang X., Qunqing L., Xie J., Jin Z.; Wang J., Li Y., Jiang K.; Fan S., (2009), Fabrication of ultralong and electrically uniform single-walled carbon nanotubes on clean substrates, *Nano Lett*. 9: 3137-41.

[2] Coleman JN., Khan U., Blau WJ., Gun'ko YK., (2006), Small but strong: A review of the mechanical properties of carbon nanotube-polymer composites. *Carbon* 44:1624-52.

[3] Fielder B., Gojny FH., Wichmann MHG., Notle MCM., Schulte K., (2006), Fundamental aspects of nano-reinforced composites.*Compos Sci Technol*. 66:3115-25.

[4] Thotenson ET.; Ren Z., Chou T-W., (2001), Advances in science and technology of carbon nanotubes and their composites: a review, *Compos Sci technol*. 61: 1899-912 .

[5] Barber AH., Cohen SR., Wanger HD., (2003), Measurement of carbon nanotube-polymer interfacial strength. *Appl Phys Lett.* 82:4140-2;

[6] Shen H.S., Zhang C.L., (2010), Thermal buckling and postbuckling behavior of functionally graded carbon naotube-reinforced composite plates, *Mater Des*. 31: 3403-11.

[7] Ma P-C., Mo S-Y., Tang B-Z., Kim J-K., (2010), Dispersion, interfacial interaction and reagglomeration of functionalized carbon nanotubes in epoxy composites. *Carbon*.48:1824-34

[8] Zhu P., Lei Z.X., Liew K.M., (2012), Static and free vibration analysis of carbon nanotube-reinforced composite plates using finite element method with first order shear deformation plate theory, *Compos struc*. 94: 1450-60 .

[9] Ke L-L., Yang J., Kitipornchai S., (2010), Nonlinear free vibration of functionally graded carbon nanotube-reinforced composite beams. *Compos Struct*. 92:676-83.

[10] Shen HS., Zhu ZH., (2010), Buckling and postbuckling behavior of functionally graded nanotube-reinforced composite plates in thermal environments. *CMC Comput Mat Contin*. 18:155-82.

[11] Esawi AMK F. M., (2007), Carbon nanotube reinforced composites: potential and current challenges, *Mater Des*. 28: 2394-401 .

[12] Fidelus JD., (2005), Thermo-mechanical properties of randomly oriented carbon/epoxy nanocomposites., *Appl Sci Manuf*. 36: 1551-61 .

[13] Shen. SH., (2009), Nonlinear bending of functionally graded carbon nanotube-reinforced composite plates in thermal environments., *Comops Struct*. 91: 9-19 .

[14] Han Y., Eliot J., (2007), Molecular dynamics simulations of the elastic properties of polymer/carbon nanotube composites, *Compt Mater Sci*. 39: 315-23 .

[15] Shooshtari M. A., (2011), Vibration characteristics of nanocomposite plates under thermal conditions including nonlinear effects, *Int J Appl Res Mech Eng*. 1.1: 60-69.

Cite this article as: M. H. Shojaeefard *et al.*: Static and modal analysis of parabolic-boundary functionalized Carbon nanotube-reinforced composite plates using FEM.
Int. J.Nano Dimens. 5(2): 187-196, Spring 2014